Accepted Manuscript

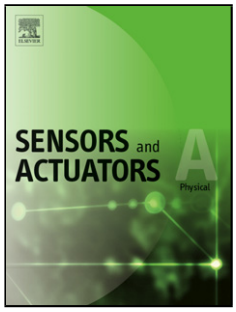

Title: Development and evaluation of an ultralow-noise sensor system for marine electric field measurements

Author: Zhendong Wang Ming Deng Kai Chen Meng Wang Qisheng Zhang Di Zeng

PII: S0924-4247(14)00151-4
DOI: http://dx.doi.org/doi:10.1016/j.sna.2014.03.026
Reference: SNA 8727

To appear in: *Sensors and Actuators A*

Received date: 6-11-2013
Revised date: 19-3-2014
Accepted date: 19-3-2014

Please cite this article as: Z. Wang, M. Deng, K. Chen, M. Wang, Q. Zhang, D. Zeng, Development and evaluation of an ultralow-noise sensor system for marine electric field measurements, *Sensors and Actuators: A Physical* (2014), http://dx.doi.org/10.1016/j.sna.2014.03.026

This is a PDF file of an unedited manuscript that has been accepted for publication. As a service to our customers we are providing this early version of the manuscript. The manuscript will undergo copyediting, typesetting, and review of the resulting proof before it is published in its final form. Please note that during the production process errors may be discovered which could affect the content, and all legal disclaimers that apply to the journal pertain.

ACCEPTED MANUSCRIPT

Development and evaluation of an ultralow-noise sensor system for marine electric field measurements

Zhendong Wang[a], Ming Deng[a,b,*], Kai Chen[a,b], Meng Wang[a,b], Qisheng Zhang[a,b], Di Zeng[a]

a *School of Geophysics and Information Technology, China University of Geosciences (Beijing), Beijing, 100083, China*

b *Key Laboratory of Geo-detection (China University of Geosciences, Beijing), Ministry of Education, Beijing, 10083, China*

* Corresponding author. Tel.: +861082320175. E-mail address: dengming@cugb.edu.cn (M. Deng).

ABSTRACT

In this paper, we describe the development of an ultralow-noise sensor system consisting of non-polarizable Ag/AgCl electrodes and a chopper amplifier for detecting marine electric field signals. Ag/AgCl electrodes were fabricated using a constant current density to clean the electrode cores and were then electrolytically chloridised by applying a constant potential. An amplifier was developed using the chopper stabilization (CHS) technique to reduce the $1/f$ noise and the initial offset. To achieve ultralow-noise performance, we took advantage of newly developed materials in the fabrication of Ag/AgCl electrodes and proposed a residual ripple reduction loop to decrease the modulated noise and the offset of the chopper amplifier. Typical measured noise levels are 0.6 nV/rt(Hz) for the Ag/AgCl electrodes and 0.55 nV/rt(Hz) for the chopper amplifier at 1 Hz. The source resistance between pairs of Ag/AgCl electrodes is approximately 5 Ω. The offset potential is typically ±0.1 mV with a drift of less than 5 μV/day. The chopper amplifier had an offset voltage below 0.2 μV with a -3 dB bandwidth from 0.01 Hz to 40 Hz and a variable gain from 80 dB to 120 dB to achieve a large dynamic range. This sensor system is used for marine electric field measurements with high precision.

Keywords: ultralow-noise; Ag/AgCl electrode; chopper amplifier; marine electric field; sensor system

1. Introduction

Marine electromagnetic (EM) methods have been used extensively over the last 10 years, including in the commercial application of marine magnetotelluric (MT) and marine controlled-source electromagnetic (CSEM) soundings for offshore hydrocarbon exploration [1,2]. Seafloor electric field measurements are essential for both the marine MT and CSEM methods. However, induction in conductive seawater attenuates the magnetotelluric fields, causing a dramatic loss of electric field power on the seafloor at frequencies greater than 1 mHz [3]. As a result, the natural marine electric field signal is similar to the noise floor of the electric fields (0.1 nV/m) at approximately 1 Hz in typical continental shelf environments. The ability to detect electric fields on the deep seafloor requires an ultralow-noise level. Thus, the noise level of the recording instrument must be sufficiently low as to not significantly distort the signals, and the instrumental resolution must be capable of providing an accurate and reliable description of these signals [4]. With an increasing number of marine electromagnetic surveys in the deep ocean, carefully designed electric field sensors and amplifiers with much lower noise levels are needed to improve detection accuracy.

Marine electric field measurements require two electrical contacts with seawater. Non-polarizable Ag/AgCl electrodes have excellent electrochemical characteristics, such as a very high ion exchange reaction current and a lack of polarization at a low current density, and are considered the optimal type of electrode for marine geophysical surveys [5]. The three classic methods for Ag/AgCl electrode construction are electrolytic, thermal and thermal electrolytic fabrication [6]. Thermal Ag/AgCl electrodes have a reversible electrochemical process and have been studied for different applications [7,8]. Ag/AgCl electrodes with less resistance at low frequencies, stable potentials and lower noise levels can be obtained using electrolytic chloriding [9]. Filloux used Ag/AgCl electrodes for the first marine MT survey and described a “water chopper” recorder to remove drift and self-potential [4]. Webb et al. designed an electrolytic Ag/AgCl electrode by applying a constant current during anodizing [10]. Constable obtained a noise level of below 1nV/rt(Hz) at 1 Hz on the deep seafloor using the same method [3,11].

ACCEPTED MANUSCRIPT

Electromagnetic Geoservices (EMGS) has used electric field sensors from Ultra Electronics, which provides various low-noise electrodes for geophysical electromagnetic surveying. Other improved approaches for fabricating Ag/AgCl reference electrodes have been studied [12-15].

To measure low-amplitude and low-frequency (0.1 Hz to 10 Hz) electrical signals using Ag/AgCl electrodes, we must develop an ultralow-noise amplifier [11]. Most amplifiers are restricted by offsets and $1/f$ noise, which dominates at low frequencies and limits the minimum detectable signal. The conventional solutions for $1/f$ noise and offset are the auto-zero (AZ), correlated double sampling (CDS) and CHS techniques [16]. AZ increases the noise density in the band above the original thermal noise floor due to aliasing or folding back of the broadband thermal noise [17]. CDS is a specific case of AZ. CHS decreases the effects of amplifier noise and offset without affecting the baseband noise floor, and has been widely used in precision amplifier design due to its low noise levels [18]. However, conventional chopper amplifiers are unable to adequately remove the ripple caused by signal demodulation which may be considered as a very low-frequency noise source. Several techniques have been proposed to eliminate these ripples, such as the resistance balancing circuit technique [19], a continuous-time AC-coupled loop [20], a combination of chopping and correlated double sampling [21] and a charge injection suppression loop [22].

In this paper, we describe a novel method to improve the performance of Ag/AgCl electrodes, including their noise level, repeatability and stability. During the anodizing process, we applied both a fixed current density and potential. A constant current density was used for cleaning to achieve a low noise level, and the constant potential was used to increase the repeatability and stability of the Ag/AgCl electrodes. We also present an ultralow-noise chopper amplifier matched with Ag/AgCl electrodes. An outer chopper with an electronic switch detector was used to reduce the modulated $1/f$ noise and offset. Data from the Ag/AgCl electrodes and chopper amplifier demonstrate their ultralow-noise performance as a result of the improved approach and the residual ripple reduction loop. This research is a significant step towards improving the noise level and resolution of seafloor electric field instruments and towards increasing the accuracy of marine electric field measurements.

2. Sensor System Description

A simplified block diagram showing the three components of the electric field signal (Ex, Ey, Ez) measurement system is given in Fig. 1. The measurement system essentially consists of an ultralow-noise sensor system and a high-precision acquisition system. As shown in the dashed box, each channel of an ultralow-noise sensor system contains two Ag/AgCl electrodes and a chopper amplifier.

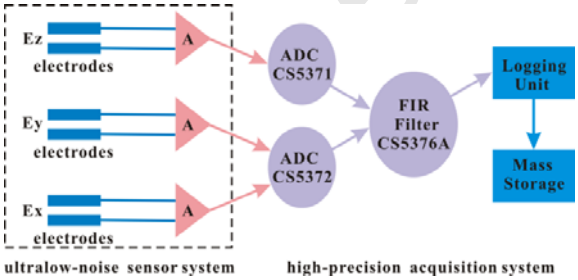

Fig. 1. A simplified block diagram of the signal measurement system. The dashed box shows the ultralow-noise sensor system.

2.1. Electrode mechanism

Ag/AgCl electrodes, which are normally represented by Ag|AgCl|C1$^-$, consist of metallic silver (Ag), solid silver chloride (AgCl) and an electrolytic solution containing a soluble chloride [6]. The reversible reaction between Ag, AgCl and the electrolytic solution can be written as

ACCEPTED MANUSCRIPT

$$AgCl + e^- \rightleftharpoons Ag + Cl^- \quad (1)$$

During measurement, small induced currents have an insignificant effect on the measured potential due to the large exchange current density.

The potential is given using the Nernst equation [9]:

$$E = E^0 - \frac{RT}{F} \ln a_{Cl^-} \quad (2)$$

where constant E^0 is the standard potential of the Ag/AgCl electrode, R is the constant of the perfect gas, T is the absolute temperature, F is the Faraday constant and a_{Cl^-} is the chloride-ion activity.

Eq. (2) shows that the potential of the Ag/AgCl electrodes is determined by the activity of the Cl^- ions. Therefore, it is necessary to maintain a constant concentration of Cl^- ions in the electrodes during fabrication.

2.2. Electrode fabrication

The fabrication of Ag/AgCl electrodes involves three main steps: (i) preparation of the electrode core, (ii) conversion of Ag to AgCl by anodization and (iii) construction of the Ag/AgCl electrode. The configuration of a cylindrical Ag/AgCl electrode is illustrated in Fig. 2.

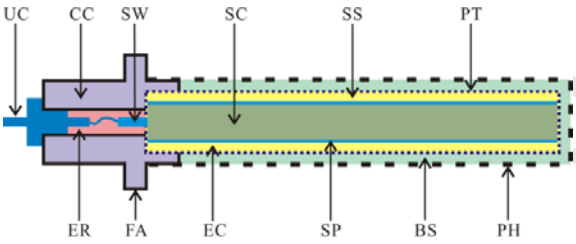

Fig. 2. Diagram of the interior of a cylindrical Ag/AgCl electrode. The electrode mainly contains electrode core (EC), cylindrical cavity (CC), fixed arm (FA), protective housing (PH) and underwater connector (UC). The electrode core is made up of silver wire (SW), porous tube (PT), silver pipe (SP) and the mixture of the silica and silver chloride powder.

Preparation of electrode cores: Prior to electrode core preparation, the materials (silver wire and silver pipe, 99.99% purity) were immersed in dilute nitric acid to remove surface contaminants and then rinsed thoroughly with deionized water. The silver wire was then connected to the top of the silver pipe with a hard link, and the bottom of the pipe was glued into a porous tube that was closed at the bottom. The interior of the silver pipe was packed with AgCl powder, and the space between the silver pipe and the porous tube was tightly packed with a mixture of AgCl and silica. The top of the porous tube was sealed with epoxy resin, completing the electrode core, and was soaked in distilled water to improve the contact.

Conversion of Ag to AgCl by anodization: The electrode core was anodized using a Source Meter Instrument (Keithley) in a 3.5% solution of NaCl at room temperature in a dark room. The electrode core was first made a cathode and another piece of silver foil (99.99% purity) was made an anode, and a constant current of 0.3 A was passed for 10 s. Then, the electrode core and silver foil were reversed, and a constant potential of 300 mV was employed for the duration of the anodization process. During electrolysis, 10~25% of the Ag underwent an anodic

ACCEPTED MANUSCRIPT

oxidation to AgCl on the surface exposed to the electrolyte, forming an AgCl layer. The chloridised electrode was then washed with distilled water.

Construction of the Ag/AgCl electrode: The underwater connector and the top portion of the electrode core were connected by a cylindrical cavity impregnated with epoxy resin to seal the connection from seawater. The electrode core was then placed inside a high-intensity cylindrical cover (ABS) that was threaded to affix it to the bottom of the cylindrical cavity. This cover, which had large holes on all sides, served as a protective housing against mechanical damage to the electrode core and was filled with a buffer substance. The fabricated Ag/AgCl electrode (as shown in Fig. 3) was stored in a sealed opaque container containing fresh 3.5% NaCl solution.

The Ag/AgCl electrodes were carefully designed during fabrication. The ions in the Ag/AgCl electrodes are in contact with the exterior medium (sea water) through a porous tube. The AgCl powder guarantees a fixed concentration of ions in the interior of the Ag/AgCl electrode, allowing the saturated solution of ions to be in contact with the silver pipe and decreasing the dissolution of the AgCl layer from the silver pipe. The cover with large holes on all sides and the buffer substance restrict the velocity of water flow through the Ag/AgCl electrode. The porous tube and the homogeneous silica can reduce the flow of water across the silver pipe. These measures avoid creating a streaming potential due to disequilibrium in the electrochemical processes acting on the Ag/AgCl electrode, thus reducing one source of noise.

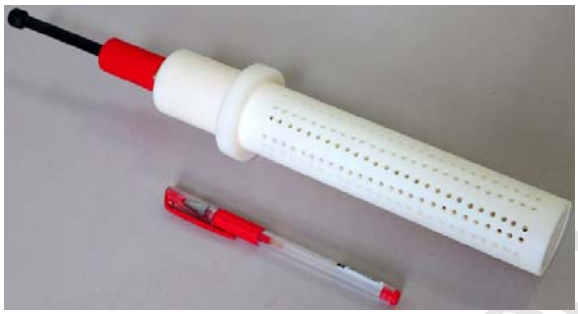

Fig. 3. Photograph of the Ag/AgCl electrode.

2.3. Amplifier principle

Fig. 4 outlines the principle of the chopper stabilization amplifier. To avoid signal aliasing, we assume that the input signals from the Ag/AgCl electrodes have a spectrum limited to half of the chopper frequency f_{chop}, and that the AC amplifier has neither noise V_n nor DC offset V_{os} [17].

As shown in Fig. 4(a), the input signals from the Ag/AgCl electrodes are first modulated by a square wave signal (duty cycle of 50%) with a chopper frequency f_{chop}. After modulation, the modulated signal with V_n and V_{os} is shifted to odd harmonics of f_{chop} and then amplified by the AC amplifier, as shown in Fig. 4(b). The output signal of the previous stage is demodulated to even harmonics, while V_n and V_{os} are modulated and shifted to odd harmonics of f_{chop}, as shown in Fig. 4(c). As a result, the spectrum of the noise is distinct from the shifted signal. Thus, the original baseband signal can be obtained without any distortion by adding a low-pass filter (LPF) after the demodulator, as shown in Fig. 4(d).

Accepted Manuscript

ACCEPTED MANUSCRIPT

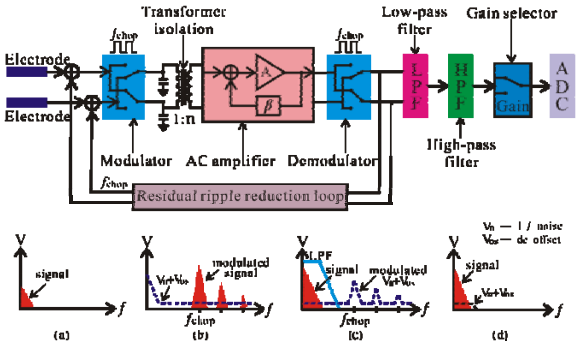

Fig. 4. Principle of the chopper stabilization amplifier. (a) The original signal; (b) the modulated signal is shifted to odd harmonics of the f_{chop}, the V_n and V_{os} appears after modulation; (c) the amplified signal is shifted to even harmonics of the f_{chop}, and the amplified V_n and V_{os} is shifted to odd harmonics of the f_{chop}; (d) the original baseband signal and the residual noise.

2.3. Amplifier design

The chopper amplifier mainly consists of a modulator, a transformer isolation stage, an AC amplifier stage, a demodulator, a residual ripple reduction loop, a LPF, a high-pass filter (HPF) and a variable gain selector. The basic structure of the chopper amplifier is shown in Fig. 4, and a photograph is given in Fig. 5.

Fig. 5. Photograph of the chopper amplifier. The input connectors match with the electrode connector.

Modulator and demodulator: The modulator consists of four Negative channel-Metal-Oxide-Semiconductor (NMOS) switches controlled by complementary clock f_{chop} with a typical resistance of 5 Ω, which avoids the introduction of additional noise. The demodulator has the same structure as the modulator. To reduce the charge injection during clock changes, the switches should be well matched to themselves and to the source resistance. The chopper frequency f_{chop} should also be carefully considered to decrease the noise and residual offset. We choose 2 kHz after considering the operational amplifier noise in the AC amplifier circuit. Fortunately, the operational amplifier has the lowest input-referred noise at this frequency.

Transformer isolation stage: The transformer isolates the Ag/AgCl electrodes, which are the only connection to the sea water and the later AC amplifier stage, thereby reducing the noise associated with the ground loops. The transformer can also match the low resistance of the Ag/AgCl electrodes and the resistance of the subsequent stage to avoid introducing additional noise. Also, the input impedance of the amplifier was designed for 1 kΩ due to the small source resistance of the Ag/AgCl electrodes. The transformer noise-matching equivalent circuit is given in Fig. 6.

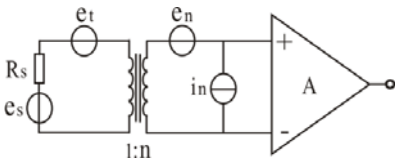

ACCEPTED MANUSCRIPT

Fig. 6. Transformer noise matching equivalent circuit model, where e_n is the amplifier voltage noise, i_n is the amplifier current noise, e_s is the signal source, R_s is the source resistance and e_t is the thermal noise of the R_s. n represents the transformer's turns ratio.

The turns ratio of the transformer is given by

$$n = \sqrt{\frac{e_n}{i_n R_s}} \tag{3}$$

AC amplifier stage: This stage contains an amplifier (A) and a feedback loop (β), as shown in Fig. 4. It is more stable as the gain is not determined by A but by β. The low-noise design of this stage must be treated cautiously because the noise in this stage dictates the overall noise of the chopper amplifier. For precise operation of the circuit, the cut-off frequency f_c of the AC amplifier must be higher than the chopper frequency f_{chop}, which allows the modulated signal to pass through this stage without distortion. The AC amplifier has an input-referred noise below 1 nV/rt(Hz) with a gain of 100.

Residual ripple reduction loop: This loop contains an outer chopper with an electronic switch detector. The f_{chop} is set to more than 10-times the input signal bandwidth to separate the undesired spectral components from the desired signals. The f_{chop} should be high enough to meet the design requirement of the LPF used to remove the unwanted tones. The final offset V'_{os} of the chopper amplifier is given by

$$V'_{os} = V_{os} \frac{f'_{chop}}{f_{chop}} \tag{4}$$

where f'_{chop} is the outer chopper frequency.

The amplifier is housed in a hermetically closed shielding box. The supply voltage of the chopper amplifier is from ±6V to ±10V. The power consumption is less than 30 mW with a supply voltage of ±6V.

3. Experiments

Measurements of the source resistance, noise, offset potential and drift of the manufactured Ag/AgCl electrodes and noise, frequency response of the chopper amplifier are described in this section, respectively.

The source resistance was measured using a micro-Ohmmeter (Agilent Technologies) on five pairs of Ag/AgCl electrodes in a 3.5% NaCl solution. To achieve an accurate resistance, a low-heat input connector and cable were used to connect the Ag/AgCl electrodes to the micro-Ohmmeter. Prior to measurement, the electrodes were immersed in the test solution for at least 48 hr to reach equilibrium.

To eliminate the influence of the voltage noise of the amplifier, we applied two independent channel measuring modes. A schematic of the measuring system is given in Fig. 7. Two Ag/AgCl electrodes immersed for at least 48 hr in a tank filled with 3.5% NaCl solution were evaluated. The voltage difference between the electrodes was increased by the amplifier. A DC nanovolt amplifier (EM Electronics) was used because of its low noise levels (equivalent noise resistance is typically 20 Ω) and its low drift (approximately one nanovolt per degree) [23]. The output of the amplifier was measured by a recorder unit (a 24-bit delta–sigma analogue-to-digital converter with sample rate of 100 Hz). The Ag/AgCl electrodes and amplifier were placed inside an aluminum container with magnetic shielding to reduce exterior interference, as shown by the dashed box in Fig. 7(a).

Accepted Manuscript

ACCEPTED MANUSCRIPT

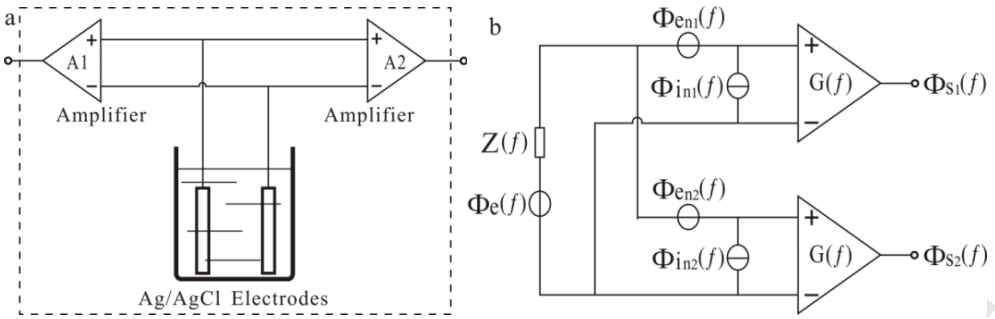

Fig. 7. (a) Noise measurement system, A1 and A2 are two identical low noise amplifiers. (b) Equivalent noise model, where e_n is the amplifier voltage noise, i_n is the amplifier current noise and e is the signal source.

As shown in Fig. 7(b), the noise at the output of the amplifiers can be expressed as

$$\Phi_{S_i}(f) = |G(f)|^2 \left\{ \Phi_e(f) + \Phi_{e_{ni}}(f) + |Z(f)|^2 \left[\Phi_{i_{n1}}(f) + \Phi_{i_{n2}}(f) \right] \right\} \quad (5)$$

The power inter-spectral density of the two output signals can be expressed as [24]:

$$\Phi_{S_1S_2}(f) = |G(f)|^2 \left\{ \Phi_e(f) + |Z(f)|^2 \left[\Phi_{i_{n1}}(f) + \Phi_{i_{n2}}(f) \right] \right\} \quad (6)$$

When $Z(f)$ is low or $\Phi_{i_{n1}}(f)$ and $\Phi_{i_{n2}}(f)$ are low, $\Phi_{S_1S_2}(f)$ can be simplified as follows:

$$\Phi_{S_1S_2}(f) = |G(f)|^2 \Phi_e(f) \quad (7)$$

where $G(f)$ is the gain of the amplifier, $\Phi_{e_n}(f)$ is the power spectral density (PSD) of the amplifier voltage noise (V^2/Hz), $\Phi_{i_n}(f)$ is the PSD of the amplifier current noise(A^2/Hz), $\Phi_e(f)$ is the PSD of the signal source from pairs of Ag/AgCl electrodes and $Z(f)$ is the resistance of pairs of Ag/AgCl electrodes.

To investigate the offset potential and drift, measurements were made using a data acquisition unit (Agilent Technologies) with a multiplexer to collect continuous data between the 21 fabricated Ag/AgCl electrodes in a tank full of 3.5% NaCl solution. One electrode was designated a reference, and the other Ag/AgCl electrodes are reported with respect to the reference. All Ag/AgCl electrodes were immersed in the test solution for at least 48 hr to establish electrochemical equilibrium before measurement. The offset potential between the Ag/AgCl electrodes and the reference electrode was measured using in-house bench link data logger software as a function of time every 20 s for 60 hr.

The noise of the chopper amplifier was measured using a low-noise, high-precision acquisition unit with 24-bit delta–sigma analogue-to-digital converter and a sample rate of 100 Hz. The chopper amplifier was placed inside a magnetically shielded aluminum container and was measured with shorted input and 5 Ω resistors. The voltage noise was measured for at least 1 hr.

The frequency response was measured using a dual phase DSP lock-in amplifier (Signal Recovery), which is ideal for determining the frequency and phase response. Frequencies from 0.001 Hz to 100 Hz were swept by the internal oscillator frequency, and the input signal magnitude and phase were simultaneously measured. The magnitude and phase were acquired as a function of the frequency using in-house software written in LabView. These measurements are made with a gain equal to 80 dB.

4. Results and discussion

4.1. Electrode source resistance

Accepted Manuscript

ACCEPTED MANUSCRIPT

The source resistance of the Ag/AgCl electrodes is not critical to the marine MT signals, although a large resistance limits the accuracy of the marine CSEM signals at higher frequencies. Therefore, the accurate determination of the Ag/AgCl electrode resistance is important, especially in the frequency range of the signals to be measured. The equivalent circuit model of the Ag/AgCl electrode consists of the spreading resistances R_s, the charge transfer resistances R_{ct} and the double-layer capacitances C_{dl} formed by the Helmholtz double-layers [9]. For simplified analysis, it can be replaced with an equivalent resistance and capacitance connected in series. Therefore, most Ag/AgCl electrodes become more capacitive with increased resistance at low frequencies.

The approximate geometric resistance of a cylindrical Ag/AgCl electrode in a solution of resistivity ρ can be given by the Dwight formula:

$$R = \frac{\rho}{2\pi c}\left(\ln\frac{2c}{a} - 1\right) \tag{8}$$

where c is the length of the Ag/AgCl electrode and a is the diameter of the Ag/AgCl electrode.

The approximate resistance R is equal to 0.794 Ω, when a cylindrical Ag/AgCl electrode in a solution with a conductivity of 4 S/m, a=10 mm and c=100 mm.

The anodizing on the electrodes and the surrounding materials are the two main factors that are mostly responsible for the increased resistance. The source resistance measurements of five pairs of Ag/AgCl electrodes are shown in Table 1.

The five pairs of Ag/AgCl electrodes produce source resistances that are approximately constant and almost independent of frequency between 0.1 Hz and 10 Hz. The source resistance of the Ag/AgCl electrode pairs is approximately 5 Ω, which is much larger than the calculated approximate geometric resistance. On the one hand, the increased resistance is mostly attributed to the resistive AgCl layer formed during the anodization process. The resistance becomes much larger when the thickness of the AgCl layer increased. It is almost certainly that too much Ag converted to AgCl will cause a large value of source resistance. It appears that approximately 10~25% of the Ag should be converted to AgCl to produce electrodes with good stability and reproducibility [6]. On the other hand, the increased resistance is may be due to the spreading resistances Rs caused by the porous tube and the protective housing, which shields the Ag/AgCl electrodes from the solution. Thus, a non-conducting material should also be carefully selected to avoid considerable impacts.

Table 1

Source resistance measurements of Ag/AgCl electrodes.

Electrodes	Resistance / Ω		
	0.1Hz	1Hz	10Hz
Pair 1	5.14	5.07	4.86
Pair 2	5.21	5.12	4.99
Pair 3	5.09	4.98	4.73
Pair 4	5.18	5.10	4.95
Pair 5	5.16	5.03	4.82

4.2. Electrode noise

It is quite difficult to measure noise level of Ag/AgCl electrode due to the noise of the amplifier and the low-amplitude signals. Accurate data can be measured only with an ultralow-noise amplifier. In this system, the DC amplifier has an ultralow-noise level of 0.45 nV/rt(Hz) in a frequency band, as shown in Fig. 8. Clearly, any measured noise is greater than the expected thermal noise associated with Ag/AgCl electrode source resistance. The noise spectrum of Ag/AgCl electrodes is composed of the thermal noise and excess noise, as follows:

ACCEPTED MANUSCRIPT

$$\Phi(f) = 4KTR(f) + af^{-n} \tag{9}$$

where a and n are constants, K is the Boltzmann constant, T is the absolute temperature and $R(f)$ is the real part of the resistance of the Ag/AgCl electrode pairs.

Fig. 8 shows that the DC amplifier noise with a shorted input is 0.45 nV/rt(Hz) at 1 Hz (as shown by the pink line) and that the DC amplifier noise with an Ag/AgCl electrodes is 0.75 nV/rt(Hz) at 1 Hz (as shown by the cyan line). Thus, the Ag/AgCl electrode noise at 1 Hz can be given by [25]

$$\sqrt{0.75^2 - 0.45^2}\ \mathrm{nV(Hz)}^{-1/2} = 0.6\ \mathrm{nV(Hz)}^{-1/2} \tag{10}$$

We also demonstrated that the noise spectrum of Ag/AgCl electrodes is limited by thermal noise from the real part of the resistance at frequencies higher than 0.1 Hz. This flat noise spectrum is mainly dependent on the surface area of the Ag/AgCl electrode. At frequencies below 0.1 Hz, we observe that excess noise varies as $1/f^n$ ($0.5<n<1.5$). This result is ascribed to the noise of electrochemical processes on the surfaces of the Ag/AgCl electrode, the long-term difference in temperature and salt concentration between the two Ag/AgCl electrodes.

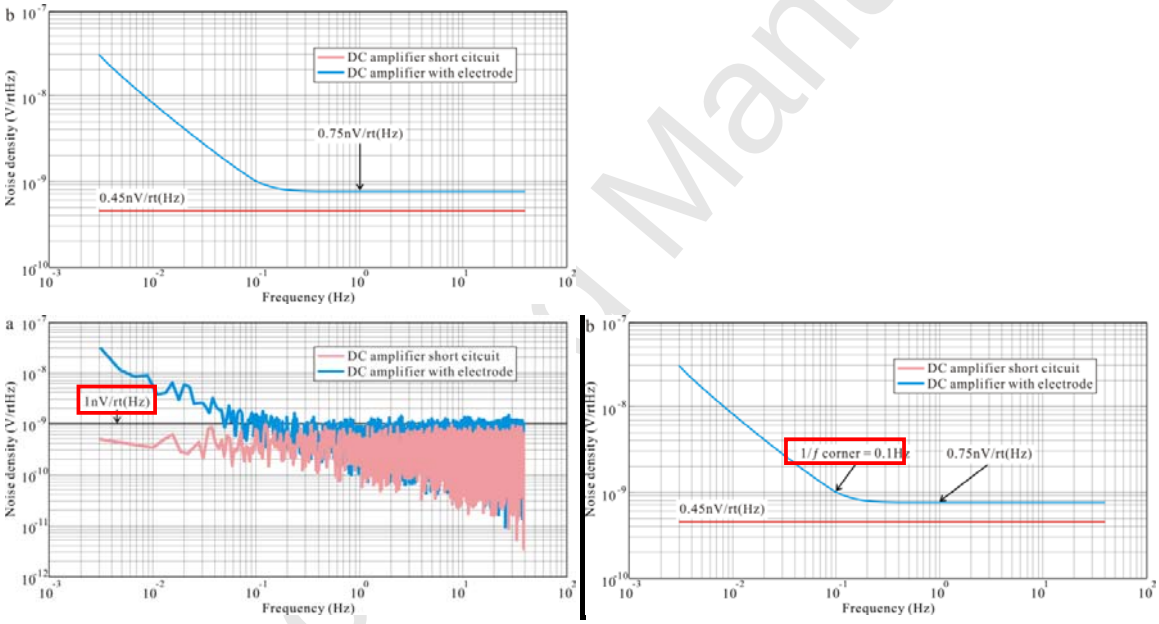

Fig. 8. Noise spectrum of the Ag/AgCl electrode and shorted DC amplifier. (a) The FFT data of the noise and (b) the calculating data using adaptive multitaper estimator of power spectral density. The $1/f$ corner frequency of the DC amplifier with electrodes is 0.1 Hz. The pink line represents the shorted DC amplifier, and the cyan line for the DC amplifier with electrodes.

4.3. Electrode offset potential

The potential across two Ag/AgCl electrodes submerged in the same solution should be zero. However, small inconsistencies due to material impurities and slight variations during fabrication create differences in the μV under zero-signal conditions. The offset potential measured over 20 Ag/AgCl electrodes is shown in Fig. 9. The measured offset potential is less than ±200 μV, and 90% of the measurements are within ±100 μV, which is smaller than previous findings [10]. The potential distribution follows an approximately Gaussian distribution. Using this information, the Ag/AgCl electrodes can be matched for the lowest available offset potential for pairs when preparing for field work. The offset potential can be minimized if great care is exercised during the fabrication of the Ag/AgCl electrodes.

ACCEPTED MANUSCRIPT

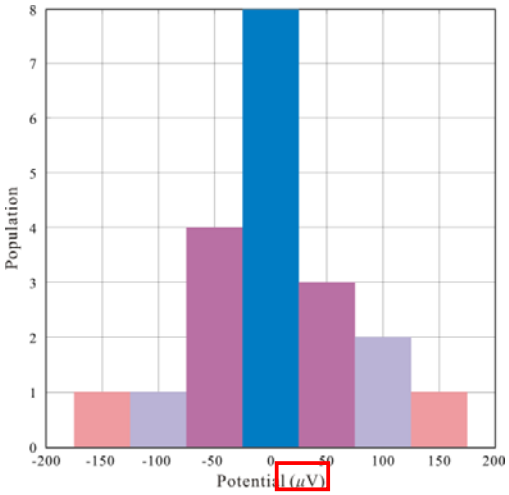

Fig. 9. Potential distribution of 20 Ag/AgCl electrodes. There are eight electrodes within ±25 μV, fifteen electrodes within ±75 μV, and eighteen electrodes within ±125 μV. Only two potential of the electrodes is greater than 125 μV.

4.4. Electrode drift

Ten Ag/AgCl electrodes are chosen at random, and their drift potential versus the reference Ag/AgCl electrode under zero-signal conditions is presented in Fig. 10. One offset potential is approximately +100 μV, and the other offset potentials are less than ±100 μV. The maximum drift is less than 20 μV over the 60-hr measurement period. The potential between the test electrodes and the reference electrode is sensitive to the ambient temperature and salinity. Most of the Ag/AgCl electrodes change uniformly when the external environment changes. This result illustrates that the performance of the Ag/AgCl electrodes is consistent. Drift also occurs until the electrodes are completely saturated (at least 48 hr) after the electrodes are put into a new solution.

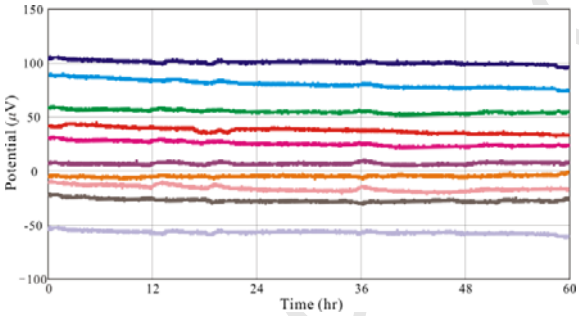

Fig. 10. Drift of 10 Ag/AgCl electrodes under zero-signal conditions. The drift of nine electrodes within ±100 μV. One electrode fluctuates around +100 μV.

One of the Ag/AgCl electrodes is depicted in Fig. 11. The offset potential is less than 10 μV, and we conclude that the drift between pairs of Ag/AgCl electrodes is less than 5 μV/day.

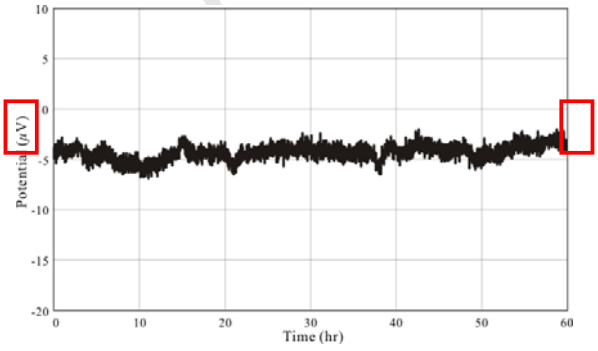

ACCEPTED MANUSCRIPT

Fig. 11. The drift of a single Ag/AgCl electrode. The offset potential is -5 μV and the variation is less than 5 μV.

4.5. Amplifier noise

Noise in the 0.1 Hz to 10 Hz interval was verified using a time-domain measurement (Fig. 12). The peak-to-peak voltage of the input-referred noise is 12 nV, and the offset voltage is less than 0.2 μV.

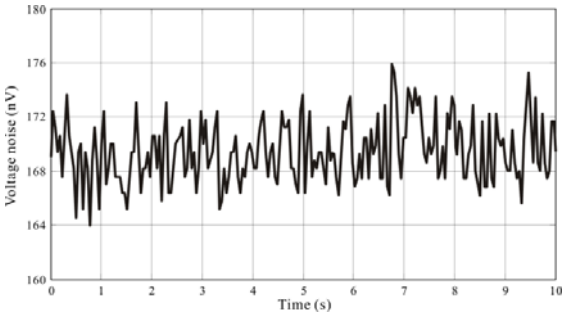

Fig. 12. Input-referred voltage noise in a 0.1-10 Hz bandwidth.

During measurement, a 5 Ω resistor was connected to the input of the chopper amplifier to evaluate the purely resistive noise level of the chopper amplifier. Fig. 13 presents the measured input-referred noise PSD of the shorted chopper amplifier voltage noise and the noise generated by a 5 Ω resistor. The noise of the chopper amplifier with a shorted circuit is 0.55 nV/rt(Hz) at 1Hz (as shown by the pink line), which is less than the calculated noise level of the Ag/AgCl electrode (see Eq. (10)). The chopper amplifier has some $1/f$ noise at frequencies below 10 mHz.

The Johnson noise of 5 Ω resistor at room temperature can be given by

$$V_R = \sqrt{4KTR} \approx 0.29\ \mathrm{nV}\left(\mathrm{Hz}\right)^{-1/2} \tag{11}$$

where K is Boltzmann's constant, T is the temperature in Kelvin and R is the resistance in ohms.

The chopper amplifier noise with the 5 Ω resistor is

$$\sqrt{0.55^2 + 0.29^2}\ \mathrm{nV}\left(\mathrm{Hz}\right)^{-1/2} = 0.62\ \mathrm{nV}\left(\mathrm{Hz}\right)^{-1/2} \tag{12}$$

This value is similar to the measured noise of chopper amplifier with 5 Ω resistor 0.64 nV/rt(Hz) at 1Hz, as shown by the cyan line in Fig. 13.

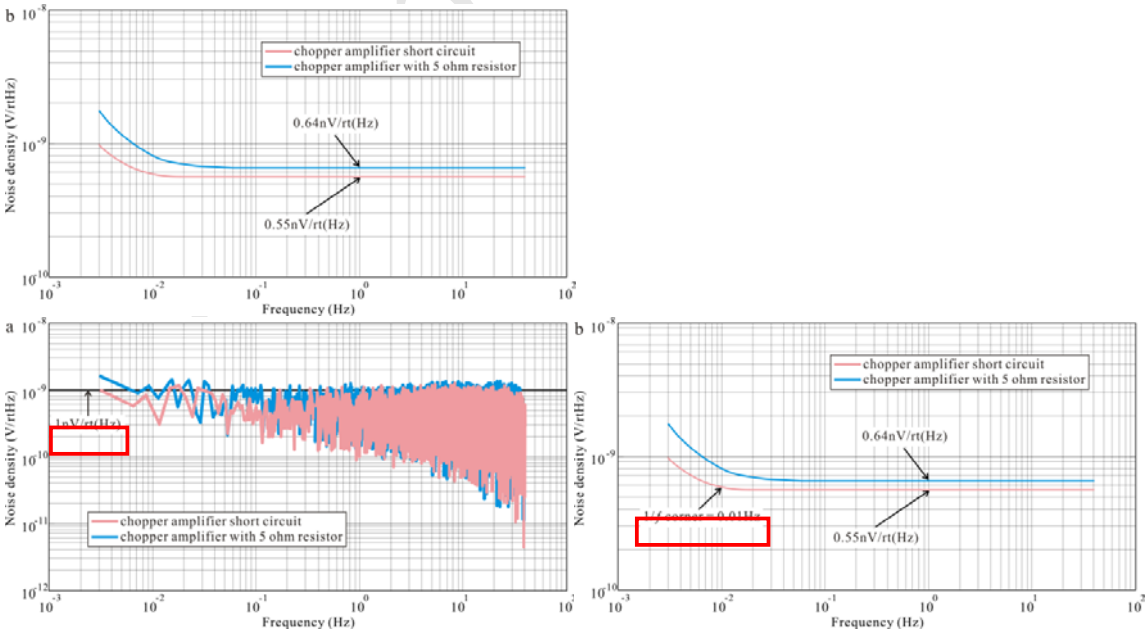

Fig. 13. Typical results for chopper amplifier voltage noise. (a) The FFT data of the noise and (b) the calculating data using adaptive

ACCEPTED MANUSCRIPT

multitaper estimator of power spectral density. The 1/f corner frequency of the shorted chopper amplifier is 0.01 Hz. The pink line represents the shorted chopper amplifier, and the cyan line for the chopper amplifier with 5 Ω resistor.

4.6. Amplifier frequency response

The chopper amplifier was designed with a variable gain from 80 dB to 120 dB to achieve a large dynamic range, a second-order LPF anti-aliasing filter at a cut-off frequency of 40 Hz and a single-pole HPF at 0.01 Hz. The measured frequency response of the chopper amplifier from 0.001 Hz to 100 Hz is given in Fig. 14. A -3 dB bandwidth from 0.01 Hz to 40 Hz is achieved with a gain of 80 dB.

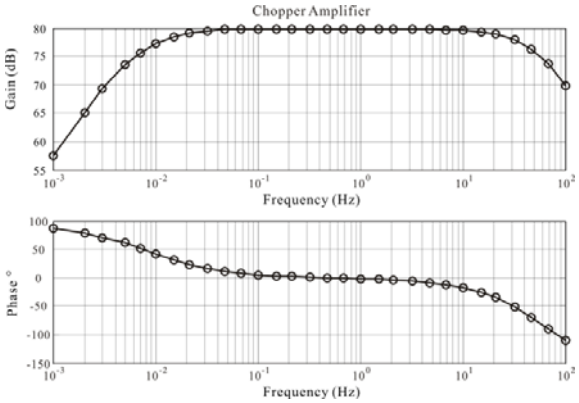

Fig. 14. Chopper amplifier frequency response. The above curve is amplitude-frequency characteristic and the following curve is the phase-frequency characteristic. The gain is 77 dB at 0.01 Hz and 40 Hz. The total gain of the chopper amplifier is 10^4.

4.7. Sensor system noise

The noise level of Ag/AgCl electrode with chopper amplifier is 1.1 nV/rt(Hz) at 1 Hz, as shown in Fig. 15. The noise of Ag/AgCl electrode at 1 Hz measured by chopper amplifier can be given by

$$\sqrt{1.1^2\text{-}0.55^2}\ \mathrm{nV(Hz)}^{-1/2} \approx 0.95\ \mathrm{nV(Hz)}^{-1/2} \tag{13}$$

This value is higher than the calculated noise level of Ag/AgCl electrode with DC amplifier (see Eq. (10)). It is ascribed to the properties of the chopper amplifier which has a higher noise floor than the DC amplifier. The corner frequency of Ag/AgCl electrode with chopper amplifier is 0.1 Hz, the same as Ag/AgCl electrode with DC amplifier. We conclude that the chopper amplifier is well matched to the Ag/AgCl electrode although the noise level of chopper amplifier is slightly higher than the ultralow-noise DC amplifier.

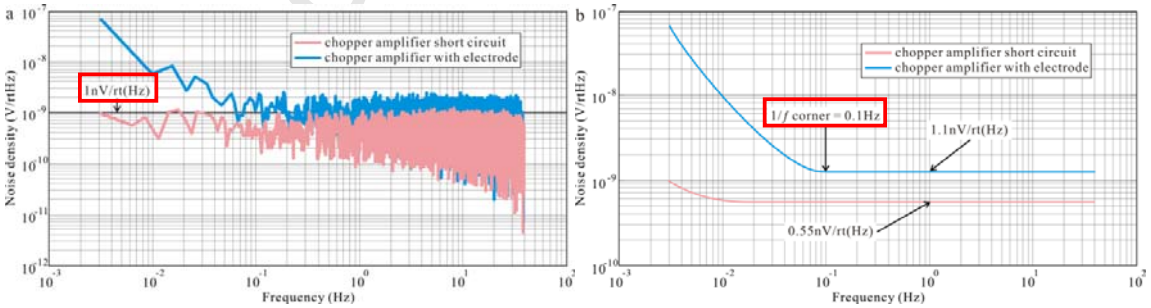

Fig. 15. Typical results for sensor system noise. (a) The FFT data of the noise and (b) the calculating data using adaptive multitaper estimator of power spectral density. The 1/f corner frequency of the chopper amplifier with electrodes is 0.1 Hz. The pink line represents the shorted chopper amplifier, and the cyan line for the sensor system.

5. Conclusions

We demonstrated a novel method for the fabrication of electrolytic Ag/AgCl electrodes for marine use.

ACCEPTED MANUSCRIPT

Compared with a constant anodizing current method, the Ag/AgCl electrodes manufactured by the novel method have a lower noise level, offset potential and drift. We can decrease the resistance between pairs of Ag/AgCl electrodes by increasing the surface area, although the surrounding materials have a large effect on the resistance. The offset and drift can be sufficiently limited to generate high-quality electrodes if the materials are carefully chosen and the fabrication is performed in a clean environment.

We designed a matching low-noise chopper amplifier for Ag/AgCl electrodes. Using a residual ripple reduction loop, an ultralow-noise level at lower frequencies and a low offset voltage were achieved. The impedance-matching transformer matches the noise between the Ag/AgCl electrodes and the chopper amplifier, thereby reducing the noise caused by ground loops. The variable gain of the chopper amplifier can be selected by the logging unit to amplify signals of different amplitudes without saturation.

We investigated an ultralow-noise sensor system for marine MT and CSEM applications. The noise level of the Ag/AgCl electrodes is 0.6 nV/rt(Hz) at 1 Hz, which is slightly higher than the noise level of the chopper amplifier with a shorted input of 0.55 nV/rt(Hz) at 1 Hz. The ultralow-noise sensor system is used for marine electric field measurements with high precision during electromagnetic prospecting.

Acknowledgments

This research was supported by The National High Technology Research and Development Program of China (863 Program) (Nos. 2009AA09A201 and 2012AA09A201).

References

[1] T. Eidesmo, S. Ellingsrud, L.M. MacGregor, S.C. Constable, M.C. Sinha, S. Johansen, F.N. Kong, H. Westerdahl, Sea Bed Logging (SBL), a new method for remote and direct identification of hydrocarbon filled layers in deepwater areas, First Break 20 (3) (2002) 144-152.

[2] S.C. Constable, Ten Years of Marine CSEM for Hydrocarbon Exploration, Geophysics 75 (5) (2010) 75A67-75A81.

[3] S.C. Constable, A.S. Orange, G.M. Hoversten, H.F. Morrison, Marine Magnetotellurics for Petroleum Exploration Part I: A Sea-Floor Equipment System, Geophysics 63 (3) (1998) 816-825.

[4] J.H. Filloux, Techniques and Instrumentation for Study of Natural Electromagnetic Induction at Sea, Physics of the Earth and Planetary Interiors 7 (1973) 323-338.

[5] R.F. Corwin, Offshore Application of Self-Potential Prospecting, Ph.D. Thesis, University of California, Berkeley, Scripps Institution of Oceanography, UC San Diego, 1973.

[6] D.J.G. Ives, G.J. Janz, Reference Electrodes: Theory and Practice, Academic Press: New York, NY, USA, 1961.

[7] D. Ming, L. Zhigang, B. Yicheng, Y. Songqing, D. Jingwu, Z. Weiguang, The Theory and Development Technology of the Sea-Floor Electric Field Sensor, Geology and Prospecting 38 (6) (2002) 43-47.

[8] W. Yunge, C. Quanxi, H. Yunxia, W. Yupeng, L. Guifang, Performance of Ag/AgCl Porous Electrode Based on Marine Electric Field Measurement, Rare Metal Materials and Engineering 41 (12) (2012) 2173-2177.

[9] A.J. Bard, L.R. Faulkner, Electrochemical Methods: Fundamentals and Applications, John Wiley & Sons, Inc: New York, NY, USA, 2001.

[10] S.C. Webb, S.C. Constable, C.S. Cox, T.K. Deaton, A Seafloor Electric Field Instrument, Geomagnetism and Geoelectricity 37 (1985) 1115-1129.

[11] S.C. Constable, Review Paper: Instrumentation for Marine Magnetotelluric and Controlled Source Electromagnetic Sounding, Geophysical Prospecting 61 (SI) 2013 1-28.

[12] P.J. Brewer, R.J. Brown, Effect of Silver Annealing Conditions on the Performance of Electrolytic Silver/Silver Chloride Electrodes used in Harned Cell Measurements of PH, Sensors 10 (3) (2010) 2202-2216.

[13] A. Crannya, N.R. Harrisa, M. Nieb, J.A. Whartonb, R.J.K. Woodb, K.R. Stokesc, Screen-printed potentiometric Ag/AgCl chloride sensors: Lifetime performance and their use in soil salt measurements, Sensors and Actuators A 169 (2) (2011) 288-294.

Accepted Manuscript

ACCEPTED MANUSCRIPT

[14] P.J. Brewer, D. Stoica, R.J. Brown, Sensitivities of Key Parameters in the Preparation of Silver/Silver Chloride Electrodes Used in Harned Cell Measurements of pH, Sensors 11 (8) (2011) 8072-8084.

[15] G. Valdés-Ramírez, G.A. Álvarez-Romero, C.A. Galán-Vidal, P.R. Hernández-Rodríguez, M.T. Ramírez-Silva, Composites: A Novel Alternative to Construct Solid State Ag/AgCl Reference Electrodes, Sensors and Actuators B 110 (3) (2005) 264-270.

[16] C.C. Enz, G.C. Temes, Circuit Techniques for Reducing the Effects of Op-Amp Imperfections: Autozeroing, Correlated Double Sampling, and Chopper Stabilization, Proceedings of the IEEE 84 (11) (1996) 1584-1614.

[17] C.C. Enz, E.A. Vittoz, F. Krummenacher, A CMOS Chopper Amplifier, IEEE Journal of Solid-State Circuits 22 (3) (1987) 335-342.

[18] A. Bakker, K. Thiele, J.H. Huijsing, A CMOS Nested-Chopper Instrumentation Amplifier with 100-nV Offset, IEEE Journal of Solid-State Circuits 35 (12) (2000) 1877-1883.

[19] P.K. Chan, J. Cui, Design of Chopper-Stabilized Amplifiers with Reduced Offset for Sensor Applications, IEEE Sensors Journal 8 (12) (2008) 1968-1980.

[20] R. Wu, K.A. Makinwa, J.H. Huijsing, A Chopper Current-Feedback Instrumentation Amplifier With a 1 mHz 1/f Noise Corner and an AC-Coupled Ripple Reduction Loop, IEEE Journal of Solid-State Circuits 44 (12) (2009) 3232-3243.

[21] M. Belloni, E. Bonizzoni, A. Fornasari, F. Maloberti, A Micropower Chopper-CDS Operational Amplifier, IEEE Journal of Solid-State Circuits 45 (12) (2010) 2521-2529.

[22] D. Drung, J.H. Storm, Ultralow-Noise Chopper Amplifier With Low Input Charge Injection, IEEE Transactions on Instrumentation and Measurement 60 (7) (2011) 2347-2352.

[23] EM DC Nanovolt Amplifier Model A10 Specification, Available online: http://www.emelectronics.co.uk/spec/A10.html.

[24] C. Gondran, E. Siebert, S. Yacoub, E. Novakov, Noise of Surface Bio-Potential Electrodes Based on NASICON Ceramic and Ag-AgCl, Medical & Biological Engineering & Computing 34 (1996) 460-466.

[25] R.B. Northrop, Analog Electronic Circuits: Analysis and Applications, Addison-Wesley: New Jersey, NJ, USA, 1990.

Biographies

Zhendong Wang was born in Shandong Province, China, in 1986. He has been pursuing the Ph.D. degree in earth exploration and information technology from China University of Geosciences (Beijing) since 2010. His main research fields are the development of geophysical instruments and low noise marine electric field measurements.

Ming Deng is a Professor in the School of Geophysics and Information Technology at China University of Geosciences (Beijing), China. He is a director of control technology and instrument department. His background is in the field of earth exploration and information technology, particularly marine electromagnetic detection technology, where he has nearly 20 years experience. His research interests cover geophysical instruments, weak geoscience signal acquisition, towed underwater observation system, deep geoelectric sensing technology, and long cycle electromagnetic measurement. In scientific research, he has participated in or hosted a number of national, provincial of major projects, and filled the electromagnetic field detection technology gaps in China for many times together with the research group of comrades. He is author or coauthor of more than 100 scientific papers and 20 patents.

Kai Chen is a lecturer in the School of Geophysics and Information Technology at China University of Geosciences (Beijing), China. He is one of the main members of the marine electromagnetic research group in China. His background is in the field of marine electromagnetic detection technology. His research interests cover weak signal acquisition, marine electromagnetic instruments development, etc.

Wang Meng is a lecturer in the School of Geophysics and Information Technology at China University of Geosciences (Beijing), China. He is one of the main members of the marine electromagnetic research group in China. His background is in the field of marine electromagnetic transmitter development. His research interests cover geophysical exploration and information technology, marine electromagnetic instruments development, etc.

Qisheng Zhang is an Associate Professor in the School of Geophysics and Information Technology at China University of Geosciences (CUGB), Beijing, China. He obtained the M.Sc. degree and the Ph.D. degree from the Geosciences University of China, Beijing, China. He has 12 years research experience in his field. His research interests include system-on-a-programmable-chip

Accepted Manuscript

ACCEPTED MANUSCRIPT

technology, measurement technology and instrument, high precision data-converters and geophysical instruments.

Accepted Manuscript

ACCEPTED MANUSCRIPT

Highlights

A novel method for fabricating Ag/AgCl electrodes with better performance is proposed.

An improved approach can reduce the modulated 1/ƒ noise and offset of the chopper amplifier.

We developed an ultralow-noise sensor system used for marine electric field measurements with high precision.

Accepted Manuscript